Starbursts: Triggers and Evolution

Shardha Jogee[1]

Division of Physics, Mathematics, and Astronomy, MS 105-24, California Institute of Technology, Pasadena, CA 91125

Abstract. Why do the circumnuclear (inner 1–2 kpc) regions of spirals show vastly different star formation rates (SFR) even if they have a comparable molecular gas content? Why do some develop starbursts which are intense short-lived ($t \ll 1$ Gyr) episodes of star formation characterized by a high star formation rate per unit mass of molecular gas (SFR/M_{H2}), which I refer to as star formation efficiency (SFE). I address these questions using high resolution ($2''$ or 100–200 pc) CO (J=1→0) observations from the Owens Valley Radio Observatory, optical and NIR images, along with published radio continuum (RC) and Brγ data. The sample of eleven galaxies includes the brightest nearby starbursts comparable to M82 and control non-starbursts. More detailed results are in [8] and [10].

1 External Disturbances and Large-Scale Stellar Bars

The sample galaxies have developed large molecular gas reservoirs of several $\times 10^8$ to several $\times 10^9\,M_\odot$ in the inner kpc radius, assuming a standard CO-to-H_2 conversion factor. As shown in Fig. 1, the circumnuclear SFR per unit mass of molecular gas spans more than an order of magnitude for a given circumnuclear molecular gas content.

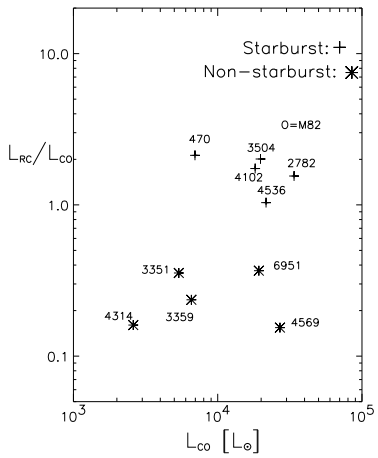

Fig. 1. The sample galaxies are shown. L_{RC} is the RC luminosity at 1.5 GHz [1] and L_{CO} is the single dish CO luminosity [14], both measured in the central $45''$.

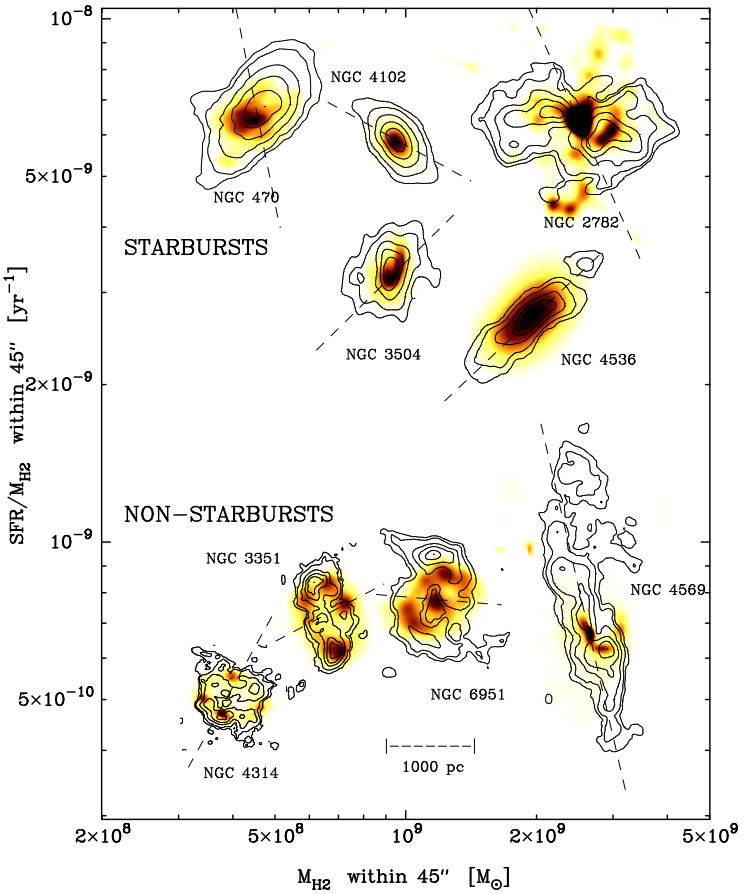

Fig. 2. In the SFR/M_{H2} vs. M_{H2} plane, the CO intensity (contours) is overlaid on the star formation (greyscale), as traced by RC in NGC 4102, NGC 2782, and NGC 6951, and by Hα in the others. The dotted line is the P.A. of the large-scale stellar bar/oval. The synthesized CO beam is typically 100–200 pc.

A spontaneously or tidally induced m = 2 instability such as a large-scale stellar bar and minor mergers/interactions can help to drive gas towards the inner kpc [6]. In optical and NIR images, all our sample galaxies show a large-scale stellar bar/oval whose position angle is marked on Fig. 2. The stellar bar may have been recently tidally triggered in NGC 3359 which has a steep abundance gradient along the bar [11], and in NGC 4569 which has a warped disk, an asymmetric bar and disturbed CO properties [8]. While the galaxies in our sample are not major mergers, all of them except for NGC 6951, show evidence for recent tidal interactions or mergers with mass ratios ranging from minor (1:10) to intermediate (1:4). NGC 2782 and NGC 470, which have the largest mass-ratio interactions, are starbursts.

The presence of a large-scale bar in starbursts and non-starbursts alike suggests that the starburst lifetime is short with respect to the timescale for bar destruction. Thus, within a given barred potential, star formation can change from an inefficient pre-burst phase in the early stages of bar-driven inflow, to a circumnuclear starburst, to a post-starburst after star formation rapidly consumes gas near the center in a few $\times 10^8$ years. The bar itself may be weakened or dissolve over timescales > 1 Gyr due to the development of a high central mass concentration (e.g., [5]; [3])

2 Morphology of the Circumnuclear Molecular Gas

What is the circumnuclear CO morphology and how does it relate to the properties of the barred potential? The molecular gas shows a wide variety of morphologies (Fig. 2) ranging from relatively axisymmetric annuli or disks (starbursts NGC 4102, NGC 3504, NGC 4536, and non-starbursts NGC 4314), elongated double-peaked and spiral morphologies (starburst NGC 2782 and non-starbursts NGC 3351 and NGC 6951) to extended distributions elongated along the large-scale bar (non-starburst NGC 4569). In NGC 4569, the gas extends out to a large (2 kpc) radius, at a similar P.A. as the large-scale stellar bar (Fig. 2), and shows complex non-circular motions. The optical, NIR, and CO properties of NGC 4569 suggest it is in the early stages of bar-driven/tidally-driven inflow of gas towards the inner kpc. In the other galaxies, the gas distribution is less extended, and in many systems it is concentrated inside the outer inner Lindblad resonance (ILR) of the large-scale bar. As shown in Fig. 3, both starbursts and non-starbursts host ILRs. In the sample, the bar pattern speed $\Omega_{\rm p} > 40$–$115\,{\rm km\ s^{-1}\ kpc^{-1}}$, the radius of the outer ILR is typically > 500 pc, and the radius of the inner IILR < 300 pc. Note that in NGC 2782 and NGC 470 which are claimed to host nuclear stellar bars [9,4], there is a strong misalignment ($\geq 40\,^\circ$) between the CO distribution and both the major axis and minor axis of the large-scale stellar bar/oval.

3 Circumnuclear Star Formation Morphology and Efficiency

The starbursts and non-starbursts have circumnuclear SFR of 3–11 and 0.1–$2\,{\rm M_\odot\,yr^{-1}}$, respectively, from RC and Brγ data. The SFE is therefore not a simple function of molecular gas content. The CO and star formation morphology are shown in Fig. 2. For a given CO-to-H_2 conversion factor, the starbursts have a larger peak gas surface density $\Sigma_{\rm gas-m}$ in the inner 500 pc radius than non-starbursts with a similar circumnuclear gas content (Fig. 4a). In the starbursts, both $\Sigma_{\rm gas-m}$ and $\Sigma_{\rm SFR}$ increase towards the inner 500 pc radius (Fig. 4a–b). Over the region of intense SF in several starbursts, $\Sigma_{\rm gas-m}$ remains close to the critical density ($\Sigma_{\rm crit}$) for the onset of gravitational instabilities [13], despite an order of magnitude variation in $\Sigma_{\rm crit}$ (Fig. 5b and e). In the non-starbursts, there

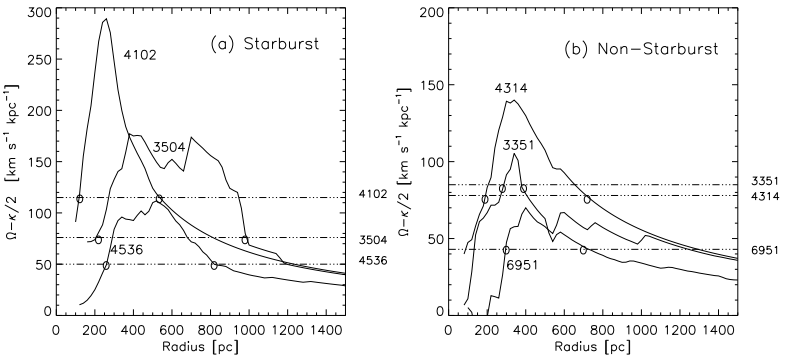

Fig. 3. $(\Omega - \kappa/2)$ is plotted against radius. The bar pattern speed $\Omega_{\rm p}$ is drawn as horizontal lines and estimated by assuming that the corotation resonance is near the end of the bar. Under the epicycle theory for a weak bar, the intersection of $(\Omega - \kappa/2)$ with $\Omega_{\rm p}$ defines the locations of the ILRs.

are gas-rich regions with no appreciable star formation, for instance, inside the ring of HII regions in NGC 3351 and NGC 4314, at the CO peaks in NGC 6951, and in the extended gas in NGC 4569 (Fig. 2). The gas surface density, although high, is still sub-critical in regions of inhibited star formation, as illustrated for NGC 4314 in Fig. 5e–f. In NGC 4569, the large local shear in the extended gas with large non-circular kinematics along the large-scale stellar bar may inhibit star formation. I suggest that circumnuclear starbursts produce a high SFE by developing supercritical surface densities in a large fraction of the gas close to the center, while sub-critical densities and large local shear may limit the SFE of non-starbursts.

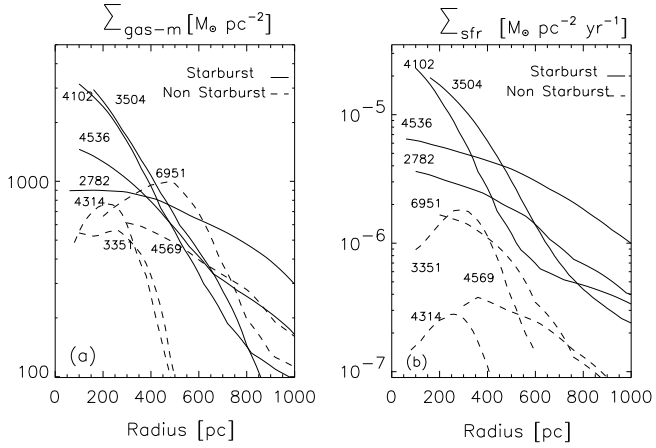

Fig. 4. (a), (b) show the azimuthally averaged molecular gas surface density ($\Sigma_{\rm gas-m}$) and SFR per unit area ($\Sigma_{\rm SFR}$). The extinction-corrected $\Sigma_{\rm SFR}$ profiles are convolved to a similar resolution of 100–200 pc for all the galaxies

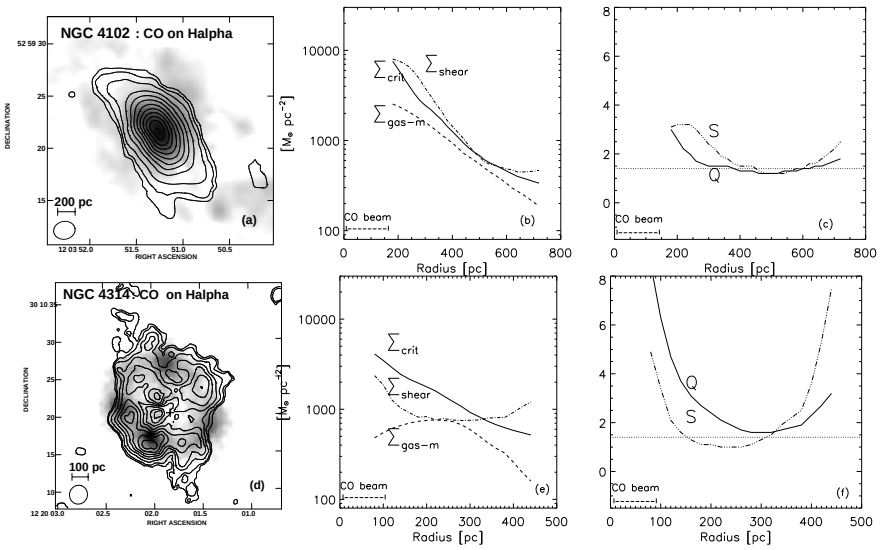

Fig. 5. **(a, d)** the CO distribution (contours) on the Hα (greyscale). **(b, e)** $\Sigma_{\rm gas-m}$, $\Sigma_{\rm crit}$, and $\Sigma_{\rm shear}$. **(c, f)** the Toomre Q and shear S parameters [8]. Quantities are plotted starting at a radius equal to the CO beam size ($\sim$2″). In the non-starburst NGC 4314, Q reaches its lowest value (1–2) in the ring of HII regions between r = 250–400 pc while at lower radii where there are no HII regions, Q increases to 6, indicating sub-critical gas densities. In the starburst NGC 4102, Q remains $\sim$1–2 between a radius of 250–700 pc, over the region of intense star formation, although $\Sigma_{\rm crit}$ varies by roughly an order of magnitude.

4 The Extreme Molecular Environment in the Inner Kpc

Table 1 illustrates how molecular gas in the inner kpc and the outer disk differ markedly. This has important implications for the circumnuclear region. First, the high molecular gas density (several 100–1000 $M_\odot$ pc^{-2}) and mass fraction (10–30%) will lead to enhanced self-gravity and clumpiness of the gas (e.g., [12]). The two-fluid disk of gravitationally coupled gas and stars will be more unstable to gravitational instabilities than a purely stellar disk (e.g., [7]). Second, in the presence of a large epicyclic frequency (several 100–1000 km s^{-1} kpc^{-1}) and velocity dispersion (10–40 km s^{-1}), gravitational instabilities can overcome Coriolis and pressure forces only at very high gas densities (few 100–1000 $M_\odot$ pc^{-2}). However, once triggered, they now grow on a timescale ($t_{\rm GI}$) as short as a few Myrs, comparable to the lifetime of an OB star. These conditions can enhance the fraction of gas converted into stars before a molecular cloud is disrupted by massive stars. Third, a high pressure, high turbulence ISM may favor more massive clusters (e.g., [2]) and it is relevant that many sample galaxies show

Table 1. Molecular Gas Properties in the Circumnuclear Region

Quantities	Outer Disk of Sa–Sc	Inner r = 500 pc of sample galaxies	Inner r = 500 pc of Arp 220
(1) $M_{gas,m}$ ($M_\odot$)	$\leq$ few $\times 10^9$	few $\times$ (10^8–10^9)	3×10^9
(2) M_{gas}/M_{dyn} (%)	< 5	10–30	40–80
(3) SFR ($M_\odot$ yr^{-1})	—	0.1–11	> 100
(4) Σ_{gas-m} ($M_\odot$ pc^{-2})	1–100	500–3500	4×10^4
(5) σ (km s^{-1})	6–10	10–40	90
(6) κ (km s^{-1} kpc^{-1})	< 100	800–3000	> 1000
(7) Σ_{crit} ($M_\odot$ pc^{-2})	< 10	500–1500	2200
(8) t_{GI} (Myr)	> 10	0.5–1.5	0.5
(9) λ_J (pc)	few $\times$ 100–1000	100–300	90

The rows are : (1) molecular gas mass (2) ratio of molecular gas mass to dynamical mass; (3) star formation rate; (4) molecular gas surface density; (5) gas velocity dispersion; (6) critical Toomre density for the onset of gravitational instabilities (7) epicyclic frequency; (8) growth timescale of the most unstable wavelength (Q/κ) (9) Jeans length

super star clusters in the inner kpc. Fourth, a comparison of Columns 3 and 4 in Table 1 suggests that the prototypical ultra luminous infrared galaxy (ULIRG) Arp 220 may be a scaled-up version of the starbursts in our sample. ULIRGs may be starbursts which have built an extreme molecular environment (density and linewidths) in the inner few 100 pc of a deep stellar potential well through major mergers or interactions.

References

1. J.J. Condon, G. Helou, D.B. Sanders, D. B., T.B. Soifer: ApJS **73**, 359 (1990)
2. B.G. Elmegreen: ApJ **411**, 170 (1993)
3. D. Friedli, W. Benz: A&A **268**, 65 (1993)
4. D. Friedli, H. Wozniak, M. Rieke, P. Bratschi: A&AS **118**, 461 (1996)
5. H. Hasan, C. Norman: ApJ **361**, 69 (1990)
6. L. Hernquist, J.C. Mihos: ApJ **448**, 41 (1995)
7. C.J. Jog: MNRAS **278**, 209 (1996)
8. S. Jogee: Ph.D. Thesis, Yale University (1999)
9. S. Jogee, J.D.P. Kenney, B.J. Smith: ApJ **526**, 665 (1999)
10. S. Jogee, J.D.P. Kenney, & N. Z. Scoville: in preparation (2001)
11. P. Martin, J. Roy: ApJ **445**, 161 (1995)
12. I. Shlosman, J. Frank, M.C. Begelman: Nature **338**, 45 (1989)
13. A. Toomre: ApJ **139**, 1217 (1964)
14. J.S. Young, S. Xie, L. Tacconi, P. Knezek, P. Viscuso, L. Tacconi-Garman, N. Scoville, S. Schneider, et al.: ApJS **98**, 219 (1995)